

University of Alabama in Huntsville

LOUIS

Honors Capstone Projects and Theses

Honors College

4-13-2017

An Analysis of the Warm-Hot Intergalactic Medium near the Coma Cluster

Casey Lanier

Follow this and additional works at: <https://louis.uah.edu/honors-capstones>

Recommended Citation

Lanier, Casey, "An Analysis of the Warm-Hot Intergalactic Medium near the Coma Cluster" (2017). *Honors Capstone Projects and Theses*. 458.

<https://louis.uah.edu/honors-capstones/458>

This Thesis is brought to you for free and open access by the Honors College at LOUIS. It has been accepted for inclusion in Honors Capstone Projects and Theses by an authorized administrator of LOUIS.

An Analysis of the Warm-Hot Intergalactic Medium near the Coma Cluster

by

Casey Lanier

An Honors Capstone

submitted in partial fulfillment of the requirements

for the Honors Diploma

to

The Honors College

of

The University of Alabama in Huntsville

April 13, 2017

Honors Capstone Director: Dr. Massimiliano Bonamente

Professor of Physics

Casey Lanier 4/17/17
Student (signature) Date

Markus Bueh April 17, 2017
Director (signature) Date

J. A. Malle 4/24/17
Department Chair (signature) Date

[Signature] 4/28/17
Honors College Dean (signature) Date



Honors College
Frank Franz Hall
+1 (256) 824-6450 (voice)
+1 (256) 824-7339 (fax)
honors@uah.edu

Honors Thesis Copyright Permission

This form must be signed by the student and submitted as a bound part of the thesis.

In presenting this thesis in partial fulfillment of the requirements for Honors Diploma or Certificate from The University of Alabama in Huntsville, I agree that the Library of this University shall make it freely available for inspection. I further agree that permission for extensive copying for scholarly purposes may be granted by my advisor or, in his/her absence, by the Chair of the Department, Director of the Program, or the Dean of the Honors College. It is also understood that due recognition shall be given to me and to The University of Alabama in Huntsville in any scholarly use which may be made of any material in this thesis.

Casey Lanier

Student Name (printed)

Casey

Student Signature

4/17/17

Date

An Analysis of the Warm-Hot Intergalactic Medium near the Coma Cluster

Casey Lanier

Abstract

I have analyzed spectra from XMM Newton data of the area around the Coma cluster, an area which is backlit by the XComae quasar, in search of absorption lines from the Warm-Hot Intergalactic Medium (WHIM). I have found only one potential absorption line, which is of limited statistical significance ($<2\sigma$), but which merits further investigation due to its correlation to other researchers' findings (Bonamente 2017a, Takei 2007). I have also established upper limits on the WHIM along the sightline, which will serve as useful constraints for future research.

1. Introduction

Only about half of all baryonic matter is contained in the galaxies, stars, nebulae, and planets that most people think of when they envision the universe. The other half is thought to be contained in the Warm-Hot Intergalactic Medium (Suárez-Velásquez 2013). The Warm-Hot Intergalactic Medium (Henceforth, WHIM) is a proposed large amount of diffuse, highly ionized gas that occupies the space between galaxies, especially around galaxy-clusters (Ren 2014). Any attempt to understand the distribution of baryons in the local universe, therefore, must include an analysis of the WHIM.

Current models put the WHIM in the $10^5 - 10^7$ K temperature range, and at about 1000 times denser than the mean universal baryonic density, (Ursino 2014) or around $N_H=10^6-10^4\text{cm}^{-3}$, where N_H is the number density of hydrogen (Takei 2007) in the Coma cluster. Due to this, the atoms are highly ionized and do not generally absorb visible light, making them effectively invisible to traditional visible-light astronomical techniques. The majority of the WHIM's interactions with the EM spectrum take place in the FUV (Far Ultra-Violet) and soft X-ray range (Ren 2014). With the launch of modern space telescopes like Chandra and XMM Newton our capacity to study these wavelengths has greatly improved but, because of the very low density nature of the WHIM, emission lines are generally too faint to be easily detectable (Nicastro 2013). In spite of this, some researchers have been able to make significant detections of emission lines from the WHIM (see Werner 2008).

Generally, a more successful approach is to look for absorption lines in areas where the WHIM is backlit by a strong FUV/X-ray source. The WHIM is not homogeneously distributed through space but is instead thought to be arranged in quasi-linear filamentary structures, often connecting galaxy clusters and other large-scale cosmic structures (Suárez-Velásquez 2013). This means that not all areas backlit by strong FUV/X-ray sources will be suitable for observing high concentrations of WHIM. A method to improve the probability of obtaining meaningful observations, as suggested by Ren (2014), is to instead use a cosmological model to find likely areas of denser WHIM presence, then to find certain ones of those areas that are also backlit by an appropriate source.

The Coma cluster ($z = .023$) is an excellent example of such a source. It is a large cluster of galaxies, which cosmological models show should be a strong indicator for the presence of WHIM (Springel, Hernquist, 2003) and is backlit by X Comae ($z = .091$), a Seyfert Galaxy or Quasar whose primary range of emissions is in the X-ray region. The Coma cluster is also suspected of having X-ray absorbing gas by prior research (Bonamente 2003). For those reasons, we have a reasonable expectation that we may find absorption lines in the X Comae spectrum where it passes near the Coma cluster. If we do not find clear signs of absorption lines, that will also give us important information. Specifically, upper limits on the density of the material can be calculated based on the observed intensity of the incident light at the wavelength of the putative absorption line.

2. Data

Our data was gathered by the XMM Newton space telescope’s Reflection Grating Spectrometer (RGS) instrument. Our data are pulled from a set of observations consisting of just over 500 ksec of exposure time. The original data was collected in six separate observations taking place between June of 2004 and June of 2006. The data was then parsed according to the standard *rgsproc* pipeline using scientific analysis software (SAS) as previously described in Bonamente (2017). After determining a level of quiescent background radiation (0.05 counts/s) using standard baseline observations, times of higher than average activity were filtered out. Because our choice of background radiation levels is fairly conservative, we are left with only just over 185ksec of clean exposure time, a drastic reduction in our quantity of data that we believe is justified by our corresponding reduced risk of false detection due to flares in the data. Table 1 details the dates and durations of our observations.

Table 1: Log of observations

Obs. ID	Start Date	Exp. Time	Clean Exp. Time
0204040101	2004-06-06	101655.8	51698.2
0204040201	2004-06-18	101857.4	37854.3
0204040301	2004-07-12	99486.3	26708.7
0304320201	2005-06-28	80647.4	40404.7
030432030	2005-06-27	55227.5	13762.7
0304320801	2006-06-06	63751.9	16946.5
Total		502626.3	187375.4

Each observation was used to generate a separate spectrum, background file, and response file; then all six spectra were then combined into one with the *rgscombine* tool. The spectra were then rebinned from 10 mÅ per data point to 20 mÅ, about three times the resolution of the RGS instrument, to increase the resolving power and the prominence of narrow line features.

Based on earlier observations, the WHIM around the Coma cluster is believed to be about 10^6 - 10^7 K (Bonamente 2003), which leads us to expect that the most abundant elements providing radiation at our wavelengths of interest will be oxygen, neon, nitrogen, and carbon ionized to the point of only having one or two electrons each (Bonamente 2017a). In this paper, I will focused on the $K\alpha$ lines of OVII, OVIII, NeIX, and NeX as they are expected to be relatively prominent and are within the range of the XMM Newton observations.

2.1 Cosmological Data

The cosmological setting I established for all of my calculations and data interpretation was developed using NASA’s *NED 1* cosmological tool. I used a Hubble parameter of $70 \text{ km s}^{-1} \text{ Mpc}^{-1}$, a Ω_m value of 0.3, and a flat universe. This produced a distance scale of $27.9 \text{ kpc arcmin}^{-1}$ at the redshift of the Coma cluster. This means that one minute of arc, which is a sixtieth of a degree, projected out to the distance of the Coma cluster covers a perpendicular distance of just over a hundred thousand light-years, or around 10^{21} meters.

3. Method of Analysis

My primary tool for analyzing the spectra has been *XSPEC*. I began by combining the spectra from each the RGS-1 and RGS-2 tools, each of which covers a different spectral range, to get a spectrum with valid data points across all of the areas of interest. I then plotted them by wavelength on a linear scale to make the data more easily readable. I then began searching for absorption lines using a line-fitting method wherein I modeled the background continuum radiation as a power law and modeled each putative absorption line as a Gaussian, which is typical of absorption lines (Nicastro 2013). Figure 1 and figure 2, seen below, show the OVII and OVIII regions of my data and model. I started by setting the power law index and normalization as free parameters, using the line energies shown in table 2, and a redshift of .0231, which is characteristic of the Coma cluster. I left the normalization parameter of the Gaussian as a free parameter. This normalization parameter will later be used in calculating maximum column densities. I also used a fixed line width of .0002 KeV for the Gaussian. This parameter corresponds to a line broadening associated with a b parameter of 100 km/s, which is a reasonable approximation, but is effectively irrelevant because the resolution of the RGS detectors is only about 50 mÅ, which is far more than our width parameter of about 10 mÅ

Fig. 1- RGS1 data of the region around the putative absorption line for OVII. Where applicable, RGS1 data is represented by the black elements on the graph and RGS2 data is in red.

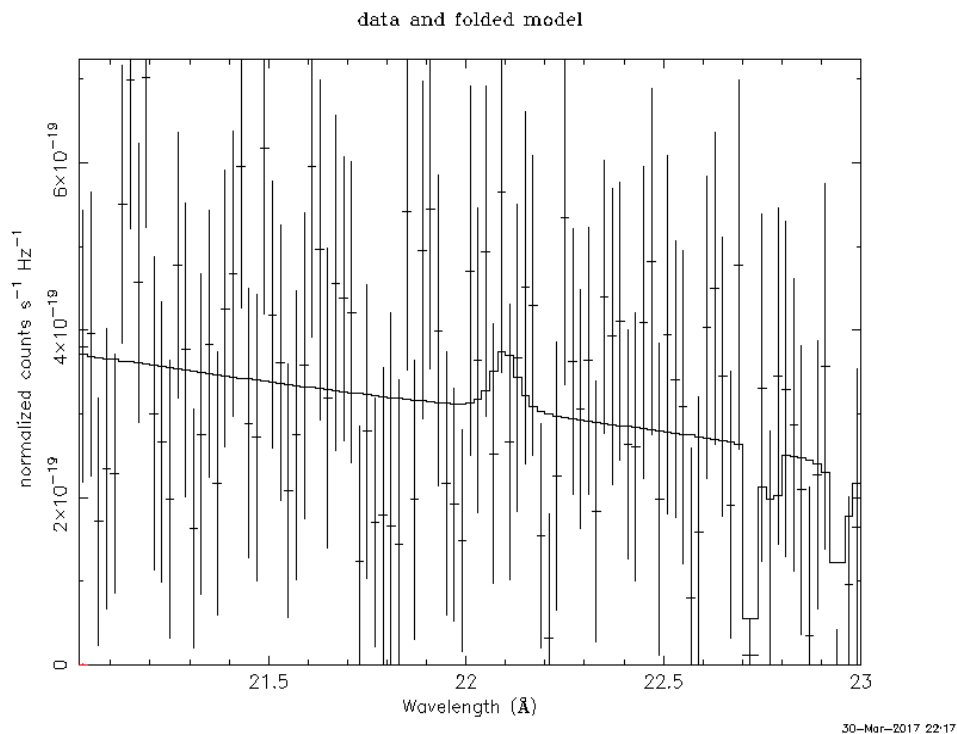
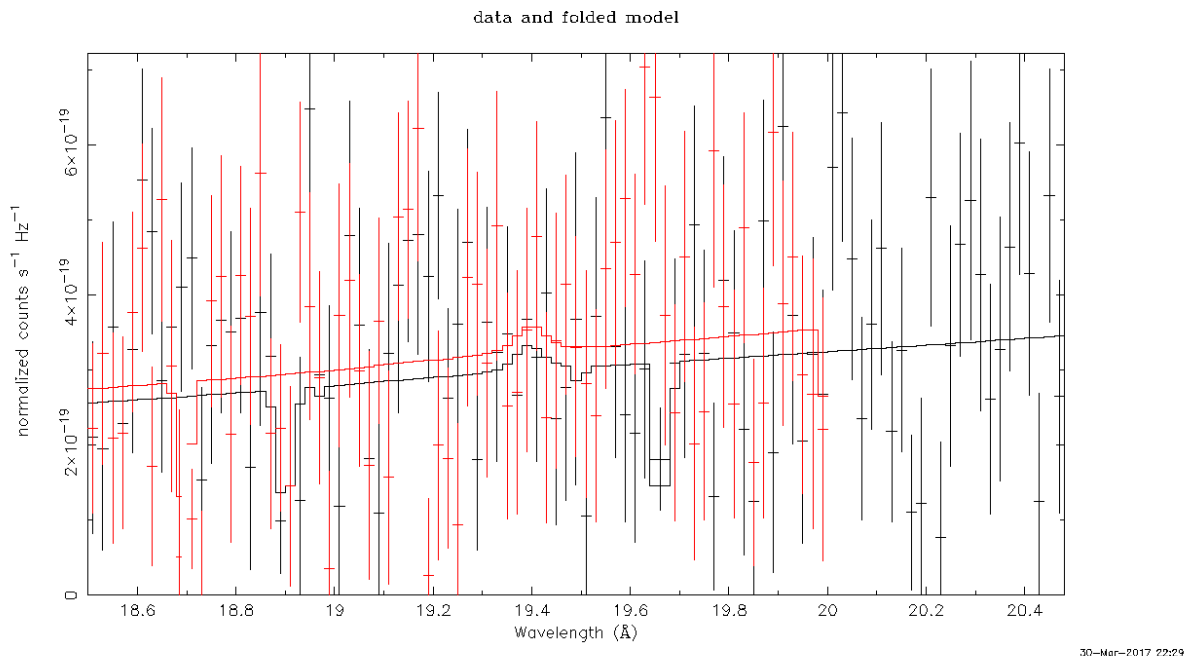


Fig. 2 – The region around the putative OVIII absorption line, which shows valid observations from both RGS instruments.



3.1 A Brief Explanation of Thermal Broadening

Thermal broadening of spectral features is caused by the random thermal motion of the putative WHIM particles being examined. Because of this random thermal motion, individual photons will be Doppler shifted into slightly different energies based on the relative velocities of the WHIM particles that they interact with. For example, an OVII ion that would ordinarily absorb light at a wavelength of 21.6 Å

Table 2 (Adapted from Bonamente 2017): Atomic parameters of $K\alpha$ absorption lines (from Verner 1996) and logarithms of Solar elemental abundances (from Anders & Grevesse 1989, relative to hydrogen).

Ion	Wavelength (Å)		Osc. strength	Solar Abundance
	Rest	$z = 0.0231$		
Ne X	12.134	12.41	0.416	-3.91
Ne IX	13.447	13.76	0.724	
O VIII	18.969	19.41	0.416	-3.07
O VII	21.602	22.19	0.696	
N VII	24.781	25.35	0.416	-3.95
N VI	28.787	29.45	0.675	
C VI	33.736	34.52	0.416	-3.44
CV	40.267	41.20	0.648	

(see table 2) but is moving towards the source of the X-rays at 100 km/s will appear to an observer who is stationary with respect to that source to instead absorb light of about 7 mÅ longer than the expected 21.6 Å. This number is calculated via the formula

$$\lambda = \lambda_0 \left(1 + \frac{v}{c}\right) \quad (1)$$

Where your difference in wavelengths is simply

$$d\lambda = \lambda_0 - \lambda \quad (2)$$

The inverse, of course, is also true for particles in random thermal motion away from the source, and accordingly the overall line width $2d\lambda$, or in this case about 14mÅ. As previously stated, because we are using observations from XMM Newton's RGS detectors which only have a spectral resolution $\sigma_\lambda = 50 \text{ mÅ}$ and in this case $2d\lambda \ll \sigma_\lambda$, the absorption line will not be clearly resolved in a typical Gaussian profile but will instead cause only a deviation from the background value in a single line element of width σ_λ (Bonamente 2017b).

3.2 Significance of Detection Calculation

The small profile of our absorption lines, coupled with the relative noisiness of our data (see Figures 1 and 2 above) makes definitive detections of absorption events very difficult. You can, however, calculate the probability that a deviation of a line element σ_λ from the model's expected value (it's ΔK) is due to a random fluctuation (noise) rather than from a genuine absorption event.

$$\Delta K = |K_{\text{model}} - K_{\text{observed}}| \quad (3)$$

I have used the built-in statistical analysis tools of *XSPEC* to calculate the goodness of fit of my additive *po+zgauss* (power law continuum + gaussian absorption) model for proposed absorption lines for each OVII, OVIII, NeIX, and NeX. The statistics associated with this goodness of fit describe the likelihood of our data representing a detection of an absorption line. The reduced χ^2 value is the sum of the variance, in terms of a number of standard deviations (σ), of the data points from the model, divided by the number of data points. More concisely,

$$\chi^2 = \sum_{i=1}^N \frac{y_i - y(x_i)}{\sigma_i} \quad (4)$$

Where N is the number of data points being examined, y_i is the value of the data point, $y(x_i)$ is the value of the line model at the wavelength of the data point, and σ_i is the value of a standard deviation.

$$\chi_{\text{reduced}}^2 = \frac{\chi^2}{N - v} \quad (5)$$

Where v is the number of free parameters, which in this case is three as described at the start of the Method of Analysis section.

The null hypothesis probability represents the likelihood of there being no relationship between the model and the observed data. A better indication, though, is the error range given in terms of standard deviation σ . Specifically, an error of 1σ represents a 68.2% probability and a 2σ error range represents a 95.4% probability. For a detection to be significant at one of these thresholds, the range of values that lie within that margin of certainty could not contain zero.

3.3 Column Density Upper Limit Calculation

When significant detections are not made at meaningful certainty levels, upper limits on the column density of WHIM along the sightline can be calculated based on the detected levels. First the equation

$$(F_\lambda)(W\lambda) = K \tag{6}$$

is used to calculate the $W\lambda$, or Equivalent Width of the absorption. The equivalent width represents the width of a rectangle with the same area as our observed Gaussian absorption line whose height is equal to the flux at the point of the model being analyzed. In this equation K is the flux as given by *XSPEC* at the point of the absorption line in question (see Table 4) and K is the normalization parameter of our Gaussian. The normalization is given with a fairly large uncertainty, which carries linearly into all future calculations made from this value. Then, taking your value of $W\lambda$ and plugging it in to the equation for column density N

$$N = 1.13 * 10^{20} \frac{W\lambda}{(\lambda^2)(f)} \frac{1}{\text{cm}^2} \tag{7}$$

Column density N is the number of particles along one square centimeter of the sight-line between the observer and the Coma cluster. λ is the redshifted wavelength of the absorption line for the ion in question, and f is the oscillator strength, as listed in Table 2. The constant is calculated from the values of fundamental constants

3.4 Extrapolation of Column Densities to Hydrogen.

Once the column density has been assigned an upper limit, you can extrapolate upper limits on the density of the WHIM overall based on those upper limits. To do this, you simply have to determine the relative abundances of the different elements to Hydrogen and Helium, which will compose the vast majority of the WHIM materials, (Ren 2014) and then apply that ratio to the solar abundance values from table 2. At that point, the matter of getting your column densities of H and He is a simple exercise in multiplication. In my calculations, I used a standard value of .1 relative solar abundance of metals as seen previously in the work of Bonamente 2017 and Ren 2014, among others.

A somewhat valid criticism of this process is that we do not actually know the relative abundance of metals in the WHIM, and that using a wrong value could illegitimatize the model of the WHIM we create with this estimate. Nonetheless, it is worthwhile to use this estimation. Because any H and He in the WHIM is completely ionized, it is effectively invisible. This makes direct detection of the H and He in a region effectively impossible, but because general consensus about the WHIM is that it is mostly primordial, it should be mostly composed of H and He. Therefore, the most useful statements you can

make are about the distribution of H and He. Because of this, we estimate the density of H using the following formula. (and a corresponding formula for He, of any other element for that matter)

$$N_H = \frac{N_{OVII}}{(f_{OVII} * A_O)} \quad (8)$$

In this example using OVII, N_H is the density of H, N_{OVII} is the density of OVII, f_{OVII} is the ion fraction of OVII, which is the portion of Oxygen present that would be in the 6th ionized state, which is dependent on temperature, and A_O is the relative abundance of O to H.

Finally, I calculated the length that the given N_H predicts for the WHIM filament. This calculation was done using

$$L_{filament} = \frac{N_H}{\rho}$$

Where ρ is the density of Hydrogen in the WHIM. The density is not known, but can be calculated based on the assumed temperature. For this paper I will use ρ values ranging from 10^{-5} to 10^{-6} cm^{-3} , which is a typical value for the WHIM and fits the probable temperature around Coma (Bonamente, 2017a)

4. Results of Analysis

I did not find any conclusive evidence of absorption by the WHIM in my data. There were no absorption signatures of either O isotope even at the 1σ level, with both models having a null-hypothesis significantly high to indicate that any apparent Gaussian features are likely only being included in the model because it was told to look for them there (See fig. 1 and fig 2). The NeX analysis showed what seemed to be an emission line (see fig. 3), but still had a fairly poor null-hypothesis probability, is significant at less than the 2σ level, and does not match up with any previously suspected features in any of the literature I have examined, and so can almost certainly be safely ignored.

The one feature that I do not believe can be fully discounted that I uncovered in my analysis is an apparent absorption line in the area expected for NeIX. The feature is significant at the 1.54σ level, and is of approximately the location and width we expected based on our thermal broadening calculations. This alone would not be enough to merit serious consideration, but it is worth noting that previous analyses of the Coma cluster have also found some evidence of this absorption line. Takei 2007 and Bonamente 2017 have both found some evidence of this same absorption, which lends some validity to an otherwise very weak observation. Bonamente 2017, however, posits that the source of this absorption is unlikely to be the WHIM due to its producing unrealistic values for the size of the filament (in excess of the length of the observable universe). Further exploration of other possible sources of this line will be necessary to uncover its cause.

Table 3: Basic redshift calculations and analysis of detection of absorption line significance for each isotope considered in this paper.

K α lines	Wavelength (Å)	Redshifted (z = .0231) Wavelength (Å)	Energy (KeV)	Reduced Chi-Squared	Null-Hypothesis	Range of 1 σ error	Range of 2 σ error	Substantial Evidence?
O VII	21.602	22.19	.574	.705	.978	-9.620 x 10 ⁻⁷ to 3.116 x 10 ⁻⁶	-1.786 x 10 ⁻⁶ to 3.940 x 10 ⁻⁶	No.
O VIII	18.969	19.41	.654	1.023	.404	-5.411 x 10 ⁻⁷ to 1.871 x 10 ⁻⁶	-1.041 x 10 ⁻⁶ to 2.371 x 10 ⁻⁶	No.
Ne IX	13.447	13.76	.92	1.342	.024	-2.549 x 10 ⁻⁶ to -3.161 x 10 ⁻⁷	-3.010 x 10 ⁻⁶ to 1.471 x 10 ⁻⁷	No.
Ne X	12.134	12.41	1.02	1.137	.174	1.289 x 10 ⁻⁷ to 3.057 x 10 ⁻⁶	-4.777 x 10 ⁻⁶ to 3.664 x 10 ⁻⁶	No

Fig. 3 – The NeX region, featuring a possible, but ignorable, emission line.

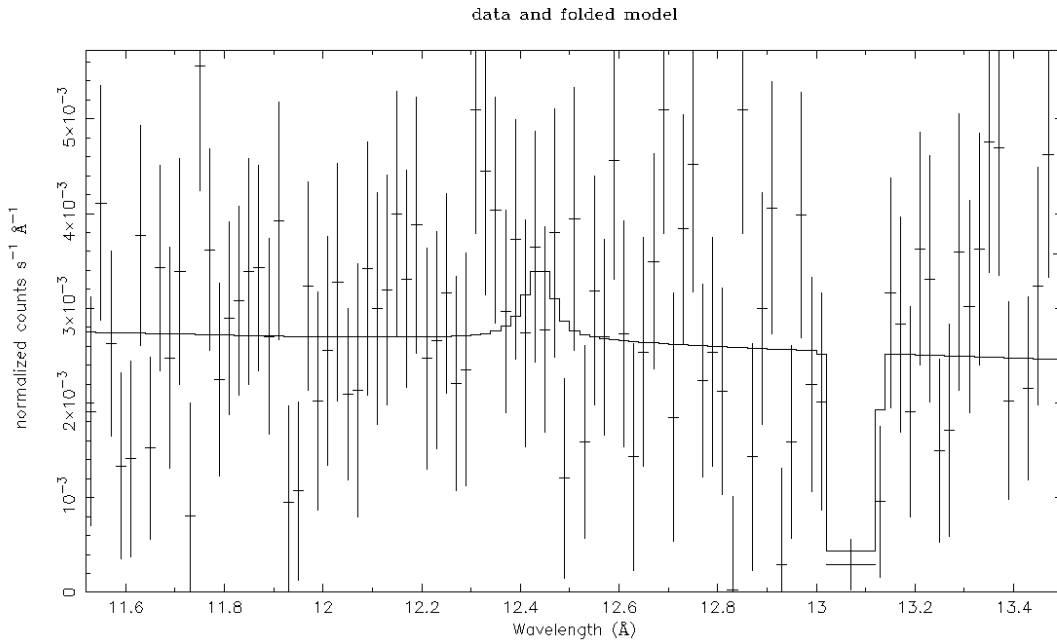
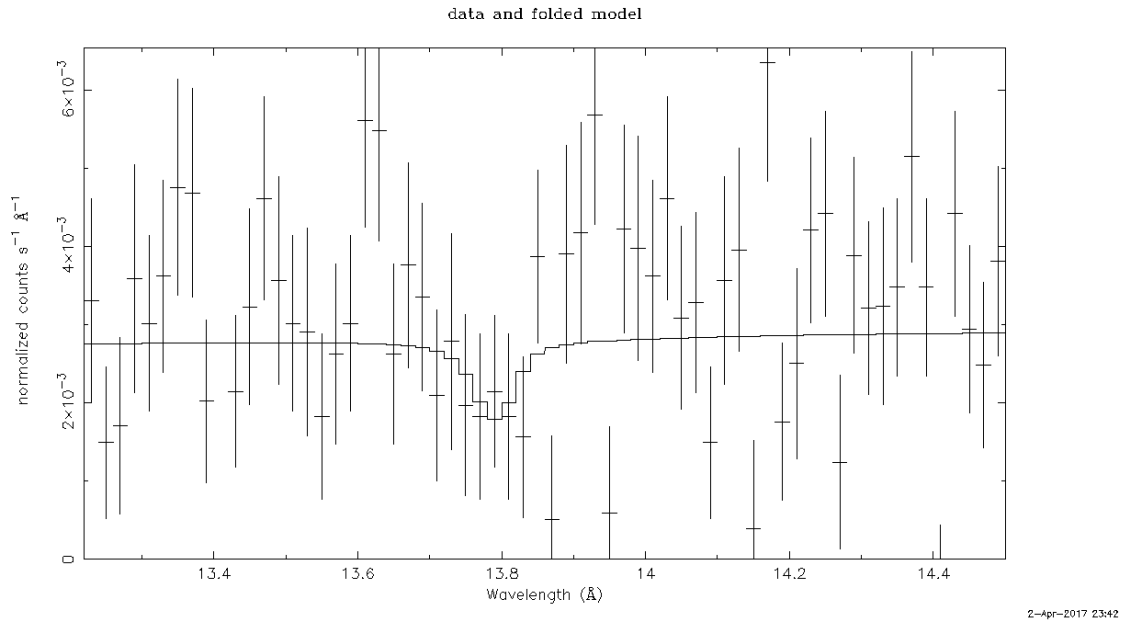


Fig. 4 – The NeIX data does show some evidence of an absorption line, but is unfortunately of $<2\sigma$ significance. The area around Ne IX contained several instrument artifacts that required the parsing out of some data.



Lacking strong evidence of absorption lines, I then went on to calculate upper limits on the column density of the WHIM in the area around the Coma cluster. These upper limits are calculated based on the idea that if there were more than a certain amount of WHIM in our area of observation, we would have made detections which would be stronger than is consistent with current data. The specific values we discovered for the column density upper limit, as well as several other related parameters, are listed in Table 4. Bear in mind that the values calculated from those column densities in the rest of this segment all represent upper limits and not true detections.

Table 4: Calculated values for the column density of each ion considered in this document, along with several other parameters used in the calculation. Many calculated parameters, such as energy width and column density, could be calculated but are meaningless in the absence of an absorption line.

K α lines	Wavelength (Å)	Redshifted (z = .0231) Wavelength (Å)	Energy (KeV)	Reduced Chi-Squared	K (1 σ uncertainty, carries into all other measurements)	EW (Angstroms)	N [Atoms(cm ⁻²)]
O VII	21.602	22.19	.57	1.17	$1.35 \times 10^{-6} \pm 2.05 \times 10^{-6}$	N/A	N/A
O VIII	18.969	19.41	.65	1.01	$5.59 \times 10^{-7} \pm 1.85 \times 10^{-6}$	N/A	N/A
Ne IX	13.447	13.76	.92	1.72	$-1.99 \times 10^{-6} \pm 1.29 \times 10^{-6}$	$4.422 \times 10^{-2} \pm 2.87 \times 10^{-2}$	$3.65 \times 10^{-16} \pm 2.37 \times 10^{-16}$
Ne X	12.134	12.41	1.02	1.13	$1.55 \times 10^{-6} \pm 1.10 \times 10^{-6}$	N/A	N/A

From the column densities of each element, I further calculated the column densities of H along the sight line as described in the Method of Analysis – Extrapolation of Column Densities to Hydrogen section. Table 5 gives the values of f_{ion} (taken from Bonamente 2017). These values are given at the 3σ certainty range, corresponding to a temperature range of $2.5 \pm .6 \times 10^6$ K. This uncertainty combines with the column density uncertainty to produce the larger uncertainty on all following values. The values for N_{H} were calculated using equation 8.

After calculating the Hydrogen column densities, I calculated the length of the filament (L_{Filament}) that would be needed to produce the given column density using equation 9. I used the densest reasonable value, 10^{-5} cm^{-3} , which produced the smallest possible length for the cloud. Using the less dense value would simply raise all length results by a factor of 10. As it stands, the calculated values are already absurdly large and there is basically no chance that any WHIM filament of that scale is responsible for this absorption. This fits with the results of Bonamente, unpublished, and is consistent with my earlier statement that this absorption is not likely caused by WHIM but merits further investigation.

Table 5: Ion fraction values based on $2.5 \pm .6 \times 10^6$ K and 3σ certainty interval, followed by N_{H} values.

Ion	f_{ion}	N_{H}	L_{filament} (cm)
O VII	.28 +.35/ -.18	N/A	N/A
O VIII	.45 +.00/ -.12	N/A	N/A
Ne IX	.93 +.05/- .13	$3.19 \times 10^{21} + 2.23 \times 10^{21}/$ -2.52×10^{21}	$3.19 \times 10^{26} + 2.23 \times 10^{26}/$ -2.52×10^{26}
Ne X	.07 +.09/- .06	N/A	N/A

5. Conclusions

Using the available data, I was able to provide generally useful limitations on the properties of the WHIM near the Coma cluster. I did not make any direct detections of significant statistical significance, however using the range of fluxes detected I was able to place informative upper limits on the amount of WHIM present in the area that could be useful to researchers in the future. I also extended these upper limits to Hydrogen. I did make a detection of Ne IX that, although not statistically significant, when combined with findings from other research could justify further investigation into the source of the possible absorption.

I would postulate that if higher resolution observations were to be made of the Coma cluster better models of the WHIM (or lack thereof) along the sightline could be made. The relative positions of XComae and the Coma cluster provide an uncommon opportunity for observing WHIM that would otherwise be detectable only by extremely faint absorption lines. Furthermore, knowing more about the WHIM near Coma could give us deeper insight into the nature of the WHIM in general, and by extension the baryonic matter of the universe as a whole. For that reason, my recommendation is that further observations be made with Chandra and perhaps HST's FUV sensors in order to better understand the WHIM of the Coma cluster.

A useful idea for further investigation of the potential Ne IX detection near Coma without the time-consuming and costly gathering of new data is re-analysis of existing data with a more sophisticated treatment of the optical nature of the WHIM in the area. For my analysis, I used a relatively simple model that assumed that the WHIM is optically thin. In other words, I assumed that the blockage of X-Rays from particles closer to XComae does not have a significant effect on the amount of light that reaches later particles. This model could be very inaccurate, especially due to the possibility of saturation, wherein all of the radiation of a certain wavelength (here 13.447 Å) is absorbed by only some of the particles and none reaches the nearer atoms. In this case, the EW is effectively capped by the limit on the amount of radiation there is to absorb, and as a result the column densities calculated will be very inaccurate. This extra depth of investigation would be time-consuming and mathematically intensive outside of the scope of this paper, but could produce superior data on the characteristics of the WHIM.

Bibliography

- Bonamente, M. *et al.* "Characterization of the warm-hot intergalactic medium near the Coma cluster through high-resolution spectroscopy of X Comae." Unpublished article. 2017a.
- . "Probability Models of Chance Fluctuations in Spectra from Astrophysical Sources". Department of Physics, University of Alabama in Huntsville. March 27, 2017b. Web.
- . *Statistics and Analysis of Scientific Data*. New York. Springer. 2013. Print.
- Leiu, R. *et al.* "The Diffuse EUV Emission from the Coma Cluster - Evidence for a Cooler Component at sub-MK Temperatures". *Science* (1996): 274. *UAH Faculty Homepage*. Web. 11 April 2017.
- Nicastro F. *et al.* "Chandra view of the warm-Hot Intergalactic Medium Toward 1ES 1553+113: Absorption-Line Detections and Identifications. I." *The Astrophysical Journal* 769 (2013): 90. *IOPscience*. Web. 11 April 2017.
- Ren, B. *et al.* "X-Ray Absorption by the Warm-Hot Intergalactic Medium in the Hercules Supercluster". *The Astrophysical Journal Letters* 782 (2014): 6. *IOPscience*. Web. 11 April 2017.
- Springel, V. Hernquist, L. "The History of Star Formation in a LCDM Universe". *Mon.Not.Roy.Astron.Soc* 339 (2003): 312. *Cornell University Library*. Web. 11 April 2017.
- Suárez-Velásquez I. F. . "The Contribution of the Warm-Hot Intergalactic medium to the cosmic Microwave Background Anisotropies via the Sunyaev-Zeldovich Effect". *Mon.Not.Roy.Astron.Soc*. Vol. 431 (2013): Pg. 342. Print. *Oxford Academic*. Web. 11 April 2017.
- Takei, Y. "The Lack of Strong O-Line Excess in the Coma Cluster Outskirts from Suzaku". *The Astrophysical Journal* 680 (2008): 2 *The American Astronomical Society*. Web. 11 April, 2017.
- *et al.* "The Warm-Hot Intergalactic Medium in Cluster Vicinities". *Progress of Theoretical Physics Supplement* 169 (2007): 29. *Oxford Academic*. Web. 11 April 2017.

Ursino, E. *et al.* "X-Ray AND Sunyaev–Zel’Dovich Properties of the Warm-Hot Intergalactic Medium". *The Astrophysical Journal* 789 (2014): 55. *IOPscience*. Web. 11 April 2017.

Werner, N. *et al.* "Detection of Hot Gas in the Filament Connecting the Clusters of Galaxies Abell 222 and Abell 223". *Astronomy & Astrophysics* Vol. 482, 2008. Pg. 29. *Astronomy & Astrophysics*. Web. 11 April 2017.